5.3 THREE BODY SCATTER SIGNATURE PRODUCING UNCERTAINTIES IN DOPPLER RADIAL VELOCITY STRUCTURES

Aurora Stan-Sion*, D. V. Carbunaru and B. Antonescu
National Meteorological Administration, Bucharest, Romanian

1. INTRDUCTION

In November 2000, the Romanian National Institute of Meteorology and Hydrology (INMH), actually the National Meteorological Administration (NMA), began to modernize the capabilities for detecting, monitoring and predicting meteorological and hydrological phenomena, by implementing the *National Integrated Meteorological System - SIMIN* project . SIMIN integrates five WSR-98D S-band radars with four existing C-band radars, to form a nine radar network (Fig. 1). The WSR-98D is a clone version of the WSR-88D systems used in the US NWS network. Currently, SIMIN produces individual site and national mosaic radar products every 6 minutes.

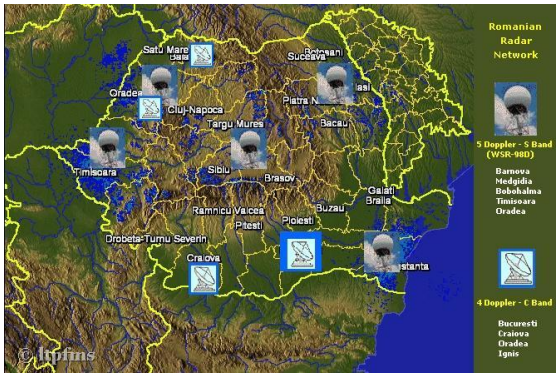

Fig. 1. The SIMIN radar network : 5 WSR-98D S-band radars (un upgraded version of WSR-88D radar used in US NWS network) and 4 C-band radars (2 from EEC – DWSR-2500C type and 2 from Gematronik – METEOR 500C type).

Advances in computer and radar technology, coupled with a dramatic increase in meteorological data sets, were not the only challenges to the forecasters. New conceptual models had to be learned and assimilated in operational practice as S-band radar allows the detection of severe weather associated with convective storms.

Thus, mesocyclones, tornadic vortex signatures (TVS), low level and mid altitude convergence zones, became "nolens volens", usual terminology in nowcasting activities, despite a general belief that tornadic storms did not occur in Romania. Observing convection in Romania through the new S-band radar network provides a sharper perspective on mesoscale environments and the storms these environments create. The highly organized convective systems, like supercells, can be better anticipated using useful radar pattern recognition software routines such as the Mesocyclone and the TVS algorithms. However, while these algorithms do demonstrate some skill they also are susceptible to radar artifacts and sampling limitations. Moreover, they sometimes fail to detect critical signatures that may be subtle or fail to meet certain thresholds. For this reason the meteorologist must carefully examine the base data to evaluate potential signature existence or non-existence.

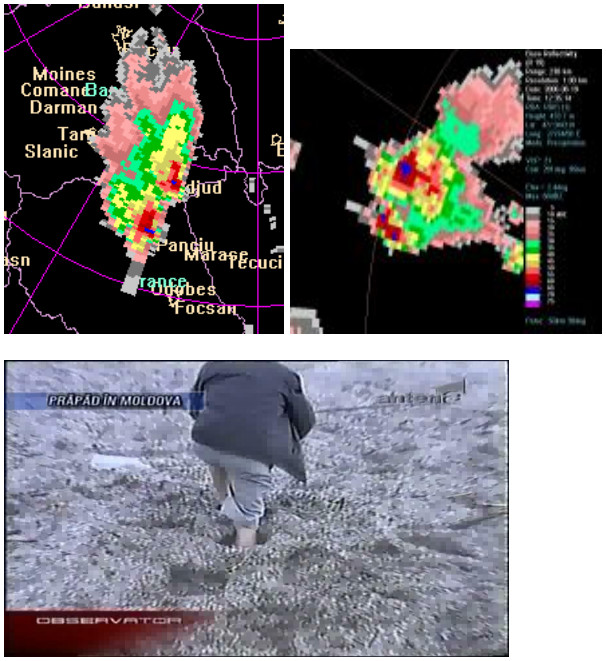

Fig. 2. First TBSS ever detected in Romania, 13 June 2004, in Moldova, upper image left, and the hail layer on the ground, image bellow. Up and right, a split storm with TBSS, on 19.06.2006 in Moldova.

* *Corresponding author address*: Aurora Stan-Sion National Meteorological Administration, Bucharest, Romania; e-mail: aurora.stan@meteo.inmh.ro .

In some of the cases radar artifacts can contaminate the reflectivity and velocity structures. For example the Three Body Scatter Signature, TBSS, can be a challenge for the operational environment.
Very soon after the completion of the radar network instalation, in 2004, the forecasters oberved several severe hail split-storms (Figure 2 up and left) that produced a layer of ice of almost 50 cm on the ground. The radar image of the storms presented a rare feature, the TBSS, never seen before on a radar screen in Romania, that helped the forecasters to issue the hail warning. When the splitting cells do not ocult eachother, is possible to detect the TBSS from each of the cells (Figure 2 up and right, from a splited storm in Moldova on 19.06.2006)
The general features of TBSS detected in Romania in 2006 are presented in Section 2. In Section 3 two cases are presented where the presence of large hail, producing TBSS, disturbed the velocity field detected by the radar. We examine a particular storm where large hail is responsible for velocity dealiasing errors that apparently lead to a false mesocyclone and tornadic vortex signature.

2. TBSS AND OPERATIONAL ASPECTS

Many studies have been made to identify how radar may be used to determine directly whether a thunderstorm contains hail. Harrison and Post (1954) reported that hail was noted in a high percentage of PPI echoes having fingerlike protrusions 1-5 miles in lenth and scallops or blunt protuberances 2-5 km from the edge of thunderstorms echoes (Fig. 3). This hailfinger can be produced by a side lobe effect and is different of the TBSS.

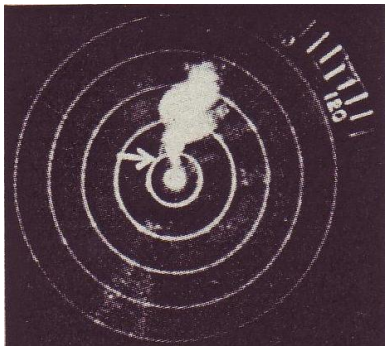

Fig. 3 – Echo associated with hail as observed with an airborne 5.5 cm radar set. The arrow points to the finger considered as an indicator of the presence of hail. [from Battan ,1959]

The TBSS was first explained by Zrnic (1987). Wilson and Reum (1988) also concluded that this radar echo artifact is the result of triple reflections, caused by non-Rayleigh radar microwaves scattering from a region of large hydrometeors, like wet hail. The triple reflections consist of: (1) a forward scattering by large hydrometeors to the ground below; (2) backscattering from the ground to the large hydrometeor region aloft, and (3) backscattering to the radar (Fig. 4). TBSS is also known as *flare- echo* (Wilson and Reum, 1988) or *hail-spike* (Zrnic, 1987), due to the appearance of the artifact in plan position indicator.

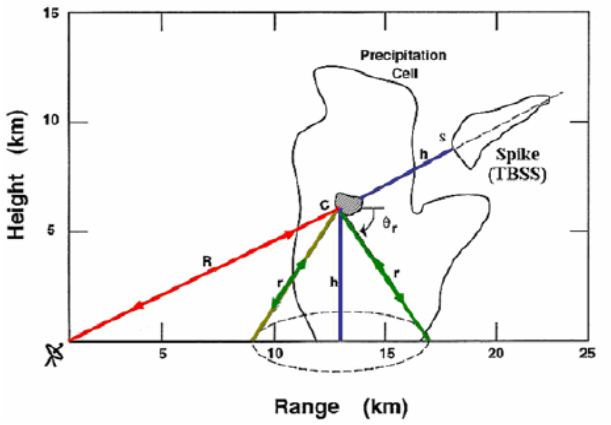

Fig. 4 - Schematic of the radar signal path responsible for the three-body spike.The dark shading near point C represents the >60 dBz core responsible for producing the artifact [adapted from Wilson and Reum (1988)].

Lemon (1978,1998) presented the TBSS and the operational application of this feature, and described some aspects of WSR-88D detection and display of the signature, correlating the TBSS with other radar characteristics of hail producer storms; he also mentioned that TBSS can mask internal storm velocities.

2.1. The TBSS case with the 8 August 2006 storm in Moldova

The first case presented was observed with Iasi radar (Fig. 5) WSR-98D S-band radar, on 8 August 2006, in the North-Eastern part of Romania, Moldova. This storm exhibited classic TBSS signatures later, at 13:27 UTC (Fig.6). The Iasi radar was operating in volume coverage pattern VCP 21 with nine elevations scans every 6-min. The first four elevations used in the operational environment are: 0.5, 1.5, 2.4 and 3.4^0.

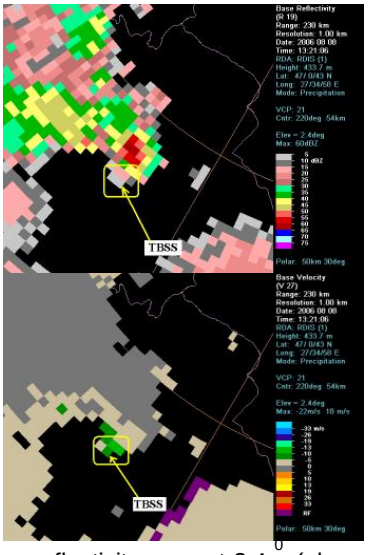

Fig. 5 - Base reflectivity scan at 2.4 ^{0} (above) and base velocity scan (bottom) from the Iasi radar at 13:21 UTC on 8 August 2006. The yellow rectangle indicates the region in which the TBSS appears.

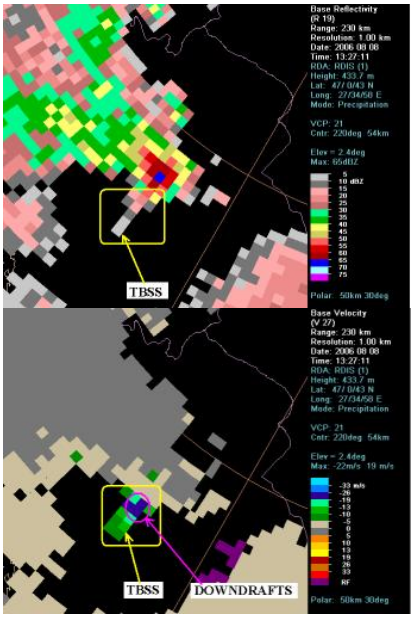

Fig. 6 - Base reflectivity scan at 2.4 ^{0} (up) and base velocity scan (bottom) from the Iasi radar at 13:27 UTC on 8 August 2006. The yellow rectangles indicate the position of TBSS. The base velocity field (right) is contaminated with negative velocities.

In order to emphasize the errors produced by TBSS, the velocity and reflectivity were represented as a function of the distance from the center of the storm (figures 7 and 8).

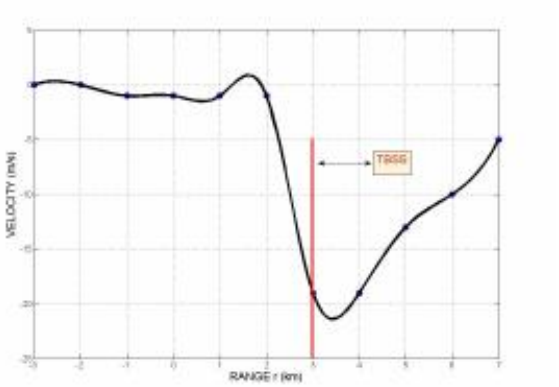

Fig. 7 – Velocity as a function of distance from the center of the storm, corresponding to the case from 8 August 2006. The velocities are measured along the TBSS at 2.4 ^{0}, starting with the closest point to the radar.

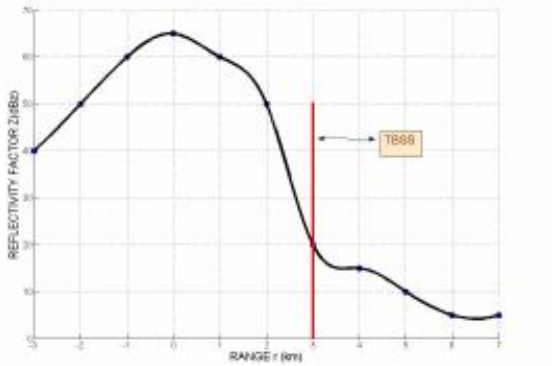

Fig. 8 – Reflectivity as a function of distance from the center of the storm, TBSS on 8 August 2006. The reflectivities are measured along the TBSS at at 2.4 ^{0}, starting from the closest point to the radar.

2.2 TBSS case on 20 May 2006 near the city of Iasi

In this case the storm produced hail stones with diameter of about 7 cm at Negresti, a village in Moldavia. The TBSS contaminates the base velocity filed with positive velocities due to the presence of a strong updraft al lower levels. This updraft promoted the growth of very large hail, and the growing hailstones have being carried across the updraft by the conserved, low-level, horizontal momentum feeding the updraft from below. For this reason the Doppler detected horizontal

positive velocities, in the hail region with a component of the low-level storm inflow. The

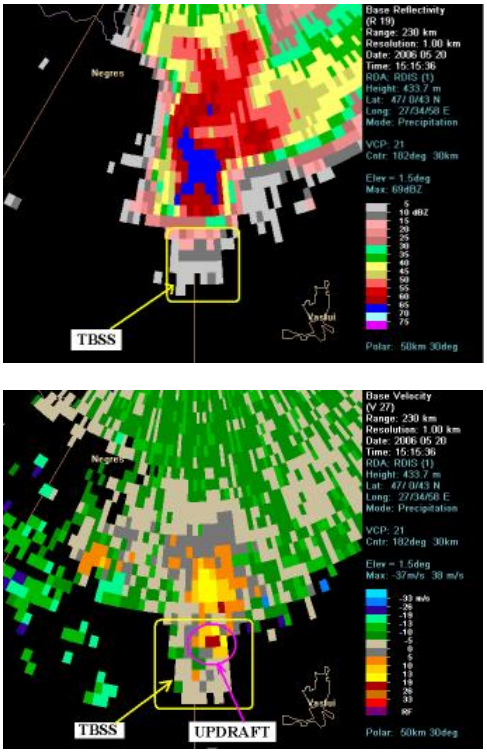

Fig. 9 – Second tilt base reflectivity scan (up) and base velocity scan (middle) from the Iasi radar at 15:15 UTC on 20 May 2006. The yellow rectangles indicate the position of TBSS. The base velocity field (middle) is contaminated with positive velocities in the spike.
The four tilts refectivities are presented in the image in the bottom.

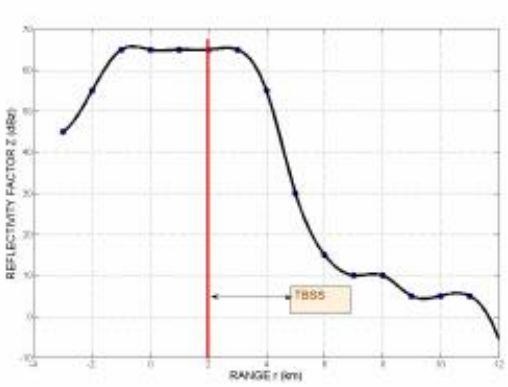

Fig. 10 – Reflectivity as a function of distance from the center of the storm, corresponding to the case from 20 May 2006. The reflectivities are measured along the TBSS, at the second tilt, starting from the closest point to the radar.

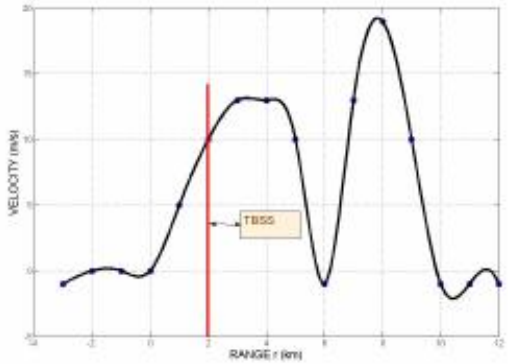

Fig. 11 – Velocity as a function of distance from the center of the storm, corresponding to the case from 20 May 2006. The velocities are measured along the radial with TBSS, starting from the closest point to the radar.

2.3 TBSS case from Baita storm, on 3 June 2006

A severe hail storm affected some villages in the central part of Romania, observed with the radar at Bobohalma, during the afternoon of 3 June 2006. described by Stan-Sion and Antonescu (2006). In the images bellow the irregular shape and structure of the hail stones can be seen.

The storm was not only a “hail monster”, but also a tornadic storm that challenged the forecaster to issue a tornado warning, which is a rare situation in Romania. The algorithms used for mesocyclones detection and tornadic vortex signature in WSR-98D are similar to those used by NEXRAD. At the fourth tilt the length of the spike was of 18 km downrange of the highest reflectivity core of 73 dBZ, situated at 4.2 km height. Along the spike the reflectivities are decreasing down to 5 dBZ, which is the threshold for reflectivity display with WSR-98 Principal User Processor. At lower elevations the length of TBSS-spike becomes shorter (10 km at 0.5º), as expected. The radial velocities at 14:54 UTC are presented in Fig. 11. The velocities associated with TBSS have negative values, but of a higher value that is usually reported in literature (Lemon, 1998). A possible explanation for this is that the large size stones reported on the ground had high terminal velocities.

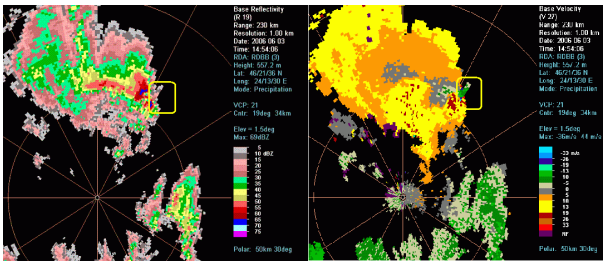

Fig. 12 Base reflectivity and base velocity at 0.5° at 14:54 UTC, 03.06.2006, WSR-98D at Iasi. The yellow rectangle indicates the position of TBSS.

In our opinion the TBSS perturbed the velocity field producing MESO and TVS structures which were unreal (seen in Fig. 13, the two MESO and TVS plotted to the North), while the mesocyclone detected to the South was consistent with radial velocities field. The supercell was moving from South-West to North-East producing a “relative to the storm” inflow in low levels oriented from North-East direction. This inbound component of the low level inflow into the storm can be a reason for the enhanced negative velocities in the TBSS spike.

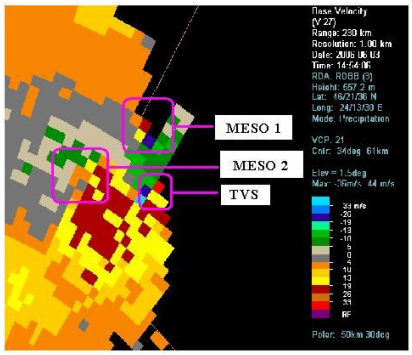

Fig. 13 - Base velocity at 1.5° at 14:54 UTC, 03.06.2006, WSR-98D at Bobohalma. The cyan rectangles enclose the MESO and TVS detected by the algorithm.

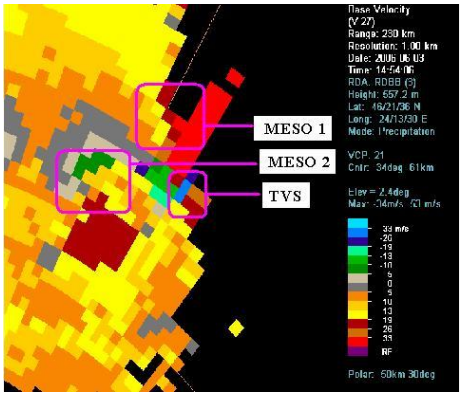

Fig. 14 - Base velocity at 2.4° at 14:54 UTC, 03.06.2006, WSR-98D at Bobohalma. The cyan lines enclose the MESO and TVS detected by the algorithm.

The storm structure shows a very strong supercell with a very well defined mesocyclone, identified corrrectly by the algorithm. However, the second mesocyclone was a false one, caused by the dealiasing failure. A closer look shows that there are real and relatively strong positive velocities that lead up to the beginning of the TBSS where sharply negative velocities begin. This very strong false convergence leads to a dealiasing failure. This strong shift may be produced by the high downward speeds of the hail stones.

The base spectrum width is quite large (Fig. 15), due to the combination between vertical falling motions of the stones and the horizontal movement near the updraft. We observed that the TBSS disturbs the velocity continuity and thus the contamination of the velocity field can be responsible for the failure of the MESO and TVS algorithms.

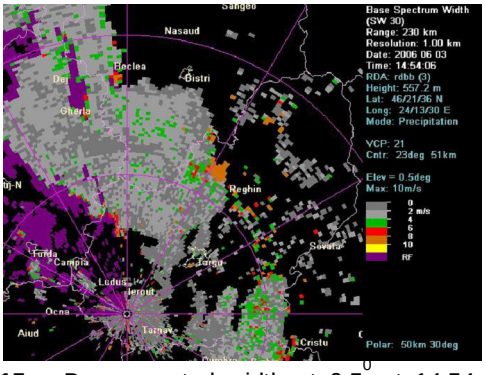

Fig. 15 – Base spectral width at 0.5° at 14:54 UTC, 03.06.2006. WSR-98D at Iasi. Large values in the centre of the image, with brown, are associated with the TBSS.

The presence of hail can produce different patterns on reflectivity or velocity . In the Fig 16. we present a case (a storm in Moldova on 19 of June 2006) where both the hailfinger-type echo and the TBSS were present.

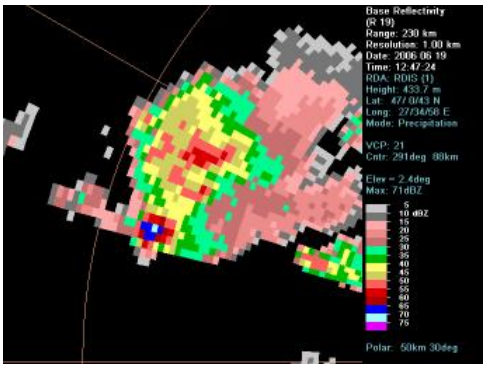

Fig. 16 TBSS and "hailfingfer-type" echo in a storm in Moldova, on 19.06.2006.

3. CONCLUSIONS

We wanted to verify if the weather detected with the S-band radars in Romania (and surroundings) shows the same characteristics as in any other places. We can say that the convection does have the same features. The Romanian experience with an S-band network, acquired in the last four years, confirms that this artifact is associated with hail reports, has the same characteristics at those reported before and does have an important operational value.

The analisys for the TBSS chracteristics was limited to one year, 2006, and in the Figure 17 we present the distribution of the TBSS recorded; we have considered only one TBSS per storm, even if it had a long life, and the position was chosen for the moment of maximum reflectivity >60 dBZ at the third tilt. The distribution was limited to the warm season (April- September) and only the very clear TBSS structures were counted (isolated storms, well observeable spikes). We mention that in the distribution of TBSS, the southern part of Romania (which is covered by 2 C-band radars), is not sampled.

A first conclusion is that the TBSS, as seen in Figure 17, is not really a rare feature in Romania.

The second conclusion refers to the climatology of "severe" hail that can be derived using radar data. The climatology of hail in Romania (unpresented here) gives a region with maximum number of "days with hail" situated over the mountains, and a lower number in the eastern part of the country, where rain is in general in deficit. However, the TBSS distribution shows that a climatology of "severe" hail, as detected with S-band radars, overlaps the regions with small number of days with hail (of any size > 6mm). It is a well known paradox that the most severe storms with severe hail form in continental climate in the regions where we would expect drought. It is also important to mention that all the TBSS cases had hail reports on the ground, but the sizes ranged from 6 mm to 9 cm.

This second conclusion pushes us to think on "conceptual models for severe hail" in the same way we were deriving conceptual models for mesocyclonic storms (Stan-Sion and Antonescu, 2006).

The TBSS (commonly called a hail spike) is widely used by operational NMA forecasters as a sufficient but not necessary indication of very large hail within a severe thunderstorm, so we could extend our analysis to all the data base (starting with 2004), considering that TBSS climatology is quite similar with severe hail climatology in the region.

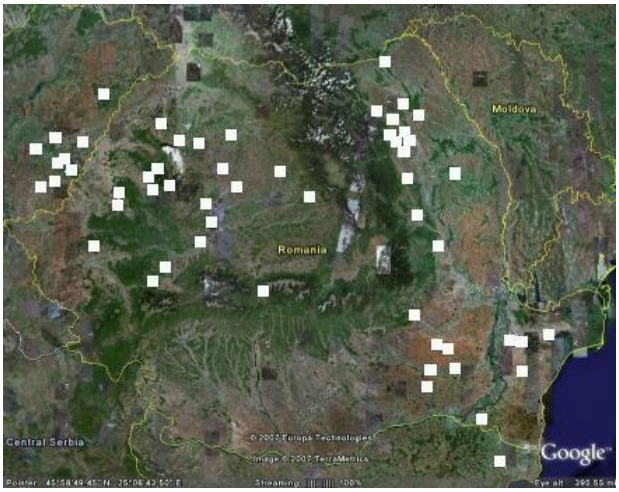

Fig. 17 – The distribution of the TBSS detected in (represented with white squares) with the SIMIN S – band radars during the warm season of 2006, in Romania.

The last conclusion is that exactly in the most difficult situations, like tracking severe convection, the forecaster should not blindly trust the algorithms.

The TBSS signature is a very important warning tool, although can not give an anticipation of more than 30' minutes since it is detected at high levels in the storm; however the hail spike can affect the radial velocities and produce disruptions in the radial velocity field that can generate unreal mesocyclonic and tornadic vortex patterns that can be artificially identified by the algorithm. In this case both severe weather, large hail and tornado, were reported at the ground and the warning was correctly issued, despite the "interference" between the TBSS and the radial velocities analyzed by the MESO and TVS algorithms. The problem will be most critical when a scanned low-level mesocyclone is immediately downrange of a hail core, which is not an unusual situation for a supercell storm. The subjective verification of the characteristic pattern of the supercell is extremely important in order to "validate" the output of the severe weather detection algorithms.

REFERENCES

Battan, L.J. 1959; Radar Observation of the Atmosphere, Univ.Chicago Press, 324 p.

Harrison, H.T., and Post, E.A. 1954: Evaluation of C-band (5.5cm) airborne weather radar. Denver, Colo.: United Air Lines, Inc.

Lemon, L. R., 1978: On the use of storm structure for hail identification. Preprints, 18th Conf. on Radar Meteorology, Atlanta, GA, Amer. Meteor.Soc., 203-206.

Lemon. L. R., 1998: The radar "Three-Body scatter Spike": An operational large-hail signature. Wea. Forecasting, **13**, 327-340

Smallcomb C., 2006: Hail spike impacts on Doppler radial velocity data during several recent lower Ohio Valley convective events. Preprints, 23rd Conference on Severe Local Storms, St. Louis, MO.

Stan-Sion, A. and Antonescu B, 2006: Radar Three Body Scatter Signature (TBSS) observed with Doppler radar network in Romania – operational aspects. Preprints, Forth European Conference on Radar in Meteorology and hydrology, Barcelona, 18-22 Sept.2006.

Stan-Sion, A. and B. Antonescu, 2006: Mesocyclones in Romania – characteristics and environments. Preprints 23rd Conference on Severe Local Storms, St. Louis, MO.

Wilson, J.B. and D. Reum, 1988: The flare echo: reflectivity and velocity signature. J.Atmos. Oceanic technol., **5**, 197-205

Zrnic, D. S., 1987: Three-body scattering produces precipitation signature of special diagnostic value. Radio Sci., **22,** 76-86.